Design, Estimation of Model Parameters, and Dynamical Study of a Hybrid Aerial-underwater Robot: *Acutus*

Ridhi Puppala, Nikhil Sivadasan, Abhijeet Vyas, Akshay Molawade,
Thiyagarajan Ranganathan and Asokan Thondiyath
Robotics Laboratory, Department of Engineering Design, Indian Institute of Technology Madras, India

Keywords: Multi Domain Vehicle, Hybrid Vehicle, Underwater Robot, Mathematical Modelling, Parameter Estimation, Dynamics.

Abstract: Design of multi-domain vehicles has been a focus in robotics research in the recent past. The objective behind developing such hybrid vehicle/robot is to combine the capabilities of systems operating in various domains. They can be of great use in numerous applications, as it maximizes the reach in multiple operation environments, especially in various challenging sectors to reduce risk to the human lives. This paper presents the design of multi-domain vehicle: a hybrid aerial-underwater robot, *Acutus*. Dynamic modelling of *Acutus* is one of the vital steps in the design process. The parameters involved in the model such as the hydrodynamic drag and added mass are critical in determining the accuracy of the model. Mathematical modelling and estimation of system parameters for *Acutus* are presented. The dynamics of the system, both in aerial and underwater domains, are initially studied individually for different possible sets of inputs. Later, simulation studies are carried out for transition between aerial and underwater domains. Preliminary mechatronic design and the experimental setup details are also presented.

1 INTRODUCTION

The major inspiration for the development of multi-domain vehicles has been from the nature. Researchers have been working on the development of bio-inspired amphibious robots capable of swimming, walking and crawling similar to snake (Crespi and Ijspeert, 2005), salamander (Crespi et al, 2013), etc. Such systems pose various challenges in terms of design and control because of the drastic variation in environment. These vehicles will be of great use in multiple applications and one such application is presented in (Michael et al., 2014) wherein, a robot which can navigate on ground and fly as well has been developed and demonstrated to be used during natural calamities like earthquake. Majority of research in design of multi-domain vehicles is concentrated on either of these two combinations: Ground-aerial or Ground-underwater. Also, for multi-domain vehicles involving operations in water, the design is majorly concentrated on surface vehicles. Another important and challenging combination is a hybrid aerial-underwater vehicle. The combination of aerial and underwater vehicles is interesting and challenging because of the very nature of operation of these systems. Inherently different properties like the density and viscosity of air and water pose challenges in the design of such robots.

A concept of aerial-aquatic vehicle with ability to traverse underwater and fly in air is discussed in (Alzu'bi et al, 2018). It uses fixed wing aerial configuration, capable of making self-propelled leaps out of water and into the air. It builds up enough speed under water to launch itself into air using a single high-speed propeller. One of the aerial-aquatic vehicles being developed uses quadrotor configuration wherein the underwater motion is achieved using an actively controlled ballast system which allows the vehicle to suspend in a horizontal position underwater at a required depth (Alzu'bi et al, 2018). A VTOL tail sitter is developed on the lines of bio-inspired cross domain vehicles which can conduct submerged operations as well as aerial flights (Stewart et al., 2018). As discussed earlier, the very nature of the domains in which the vehicles are to be operated, demands intense design and simulation analysis before it is fabricated.

Modelling of underwater systems involve a whole lot of unknown variables, which needs to be estimated. Some of the critical parameters to be

Puppala, R., Sivadasan, N., Vyas, A., Molawade, A., Ranganathan, T. and Thondiyath, A.
Design, Estimation of Model Parameters, and Dynamical Study of a Hybrid Aerial-underwater Robot: Acutus.
DOI: 10.5220/0007926104230430
In *Proceedings of the 16th International Conference on Informatics in Control, Automation and Robotics (ICINCO 2019)*, pages 423-430
ISBN: 978-989-758-380-3

estimated are the hydrodynamic derivatives, rigid body and added mass coefficients. Modelling of underwater systems have already been attempted countless times in the past (Szymak, 2016), (Wang et al., 2009), (Ai et al, 2018). Modelling of conventional aerial multirotor systems are comparatively easier, as most of the parameters can be directly obtained from CAD models. Experimentally verified models of the two popular UAV configurations, the fixed wing (Khan and Nahon, 2016), (Bouabdallah and Siegwart, 2006) and VTOL (Fernando et al, 2013) can be adopted to model similar configurations. (Zhang et al., 2014) and (Kurak and Hodzic, 2018) discuss and review all the existing popular quadrotor dynamics modelling methods.

Estimation of parameters involved in the mathematical model is the next vital step in modelling a system. Some of estimation methods use a linear approximation of the mathematical model of the system, which then gives a least squares optimal estimation of the parameters, using the Moore Penrose Inverse method (Caccia et al, 2000). Sensory instrumentation to measure the acceleration of underwater systems is still not standardised and calculation of acceleration by integrating velocity may be erroneous. A low pass-filtering technique like those discussed in (Wales, 1986), (Iisu et al., 1987) and (Slotine and Li, 1989) may be required to estimate the parameters numerically. (Smallwood and Whitcomb, 2003) introduces a stable online adaptive framework for the estimation of parameters. (Ranganathan et al., 2018) introduces a different method which makes use of concepts from both least square method and free decay tests. The least square sum (integral) of the error is minimised using a gradient descent method.

In this paper, we propose the design of a hybrid vehicle, *Acutus*, which is a fish-shaped aerial-underwater vehicle that uses quadrotor for aerial navigation and underwater thrusters for propulsion in water. Underwater motion is achieved using a single water thruster along with actuated control planes as flaps and rudder. The presented model is capable of independent manoeuvres in both aerial and underwater environments. The quadrotor is enabled over a switching mechanism wherein the quadrotor arms can be retracted while diving underwater.

2 CONCEPTUAL DESIGN AND WORKING PRINCIPLE

The conceptual CAD design of *Acutus* with right-hand global frame co-ordinates O_G: $\{X_G, Y_G, Z_G\}$ and body frame co-ordinates O_B: $\{X_B, Y_B, Z_B\}$ are shown in Figure 1. Body frame origin (O_B) is fixed to centre of gravity (COG). The balance between weight and buoyancy of *Acutus* is critical and the vehicle is designed to be slightly positively buoyant (1N). The flexibility in design is greatly narrowed down by the intersection of constraints like the volume of underwater capsule, weight during aerial flight and structural integrity against underwater pressure. The proposed design has an outer profile, best approximated to the form of a fish. The streamlined outer profile helps overcome the hydrodynamic drag. Furthermore, design is conceptualized in such a way that it minimizes the drag in aquatic medium by minimal exposure of redundant extended surfaces against the flow. Since the vehicle is designed to be positively buoyant, the thrust required to dive-in should be more than the residual buoyancy (difference between weight and buoyancy). Hence, there is also a need to regulate the weight and buoyancy of the system while ensuring power efficient use of thrusters.

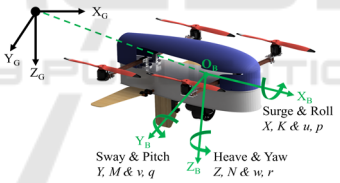

Figure 1: Isometric view of *Acutus*.

The proposed model is a reconfigurable system which switches from aerial configuration to underwater configuration while entering water by retracting the arms having aerial propellers. The mechanism proposed for retraction of arms is a double worm-drive arrangement, which actuates two arms at the same time as shown in Figure 2. Worm-drive mechanism ensures rigidity and non-back drivability during underwater operation. The mechanism is light and compact and allows sequential retraction of both pair of arms while avoiding collision.

Acutus is designed to have four controllable, coupled degrees of freedom. The surge motion is generated by a water thruster. Pitch is a coupled degree of freedom achieved by vectoring the surge velocity using the two flaps connected on either side of the metallic body. Yaw can be achieved by

controlling the rudder connected right behind the thruster. Roll is passively stabilized and heave is achieved by coupling pitch along with surge.

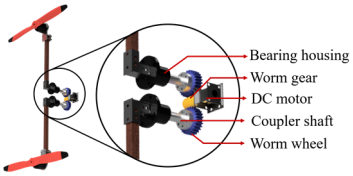

Figure 2: Worm drive for retraction of quad rotor arms.

It is worthwhile to notice that most of the degrees of freedom are coupled for underwater operation. During navigation in air, the arms with aerial propellers are extended. This allows *Acutus* to manoeuvre in air with 4 degrees of freedom viz. heave, yaw, pitch and roll. Once the air-water interface is reached, the arms are retracted within the body before diving inside water in order to minimize the drag forces due to unnecessary extended parts of the vehicle. The mass of the vehicle is distributed in such a way that the vehicle rests with a slight pitch at the transition stage (floating at the air-water interface). This pitch helps the vehicle to dive in completely when the thruster is turned on. Later by controlling the right and left flaps, required pitching motion is achieved. The aerial rotors are mounted such that if the vehicle comes back at the air-water interface, all the 4 air propellers lie outside water and can be actuated to escape out of the water medium.

3 ESTIMATION OF MODEL PARAMETERS AND DYNAMICS

A mathematical model of the underwater and aerial system has been developed to perform a detailed analysis of the overall system at different operating conditions. The 6 DOF underwater dynamics has been subdivided into dynamics of fuselage and dynamics of control planes and thruster.

3.1 Parameter Estimation for Fuselage Dynamics

Fuselage of vehicle consists of the metallic body and shroud. The Newton-Euler formulation is used in modelling the dynamics of fuselage (Fossen, 2011). The velocities, forces, and moments in body fixed and earth fixed frame and the global pose are represented based on SNAME convention (Fossen, 2011).

$$\begin{gathered} \boldsymbol{M\dot{\nu} + C(\nu)\nu + D(\nu)\nu + g(\eta) = \tau} \text{ where,} \\ \boldsymbol{M = M_{RB} + M_a} \\ \boldsymbol{C(\nu) = C_{RB}(\nu) + C_a(\nu)} \\ \boldsymbol{D(\nu) = D_L(\nu) + D_Q(\nu)} \end{gathered} \quad (1)$$

The governing equation for overall dynamics of underwater system is given in (1) has been implemented in MATLAB Simulink. $\boldsymbol{\eta}$ is global pose vector, $\boldsymbol{\nu}$ is body frame velocity vector and $\boldsymbol{\tau}$ is a vector of forces and moments of dimensions 6×1. Earth frame velocities can be computed from body frame velocities using the kinematic transformation $\boldsymbol{\dot{\eta} = J(\eta)\nu}$ where $\boldsymbol{J(\eta)}$ is the Jacobian matrix.

We employ computational methods to estimate the model parameters. Mass matrix ($\boldsymbol{M}$) is sum of rigid body inertial matrix ($\boldsymbol{M_{RB}}$) and added mass matrix ($\boldsymbol{M_a}$). Coriolis and Centripetal forces matrix $\boldsymbol{C(\nu)}$ can be expressed as a sum of rigid body and added mass terms as shown in (1). The elements of the matrices $\boldsymbol{M_{RB}}$ and $\boldsymbol{C_{RB}(\nu)}$ are estimated from 3D CAD model. $\boldsymbol{M_a}$ and $\boldsymbol{C_a(\nu)}$ are estimated by approximating the metallic body to standard geometry. Current prototype is approximated to a cylinder of same volume with the same length as real prototype and diameter of 60*mm*. Damping matrix $\boldsymbol{D(\nu)}$ is square matrix consisting of linear and quadratic hydrodynamic drag coefficients. Restoring forces and moments vector $\boldsymbol{g}$ is a function of $\boldsymbol{\eta}$ capturing the effects of gravity, buoyancy, centre of gravity (COG) and centre of buoyancy (COB) on the body.

The linear and quadratic damping terms are estimated from fluid flow analysis of the fuselage using Computational Fluid Dynamics (CFD). CFD simulations were performed for 10 equally spaced linear velocities in the range of -0.5 to 0.5*m/s* along X_G, Y_G, Z_G axes, and similarly for rotational velocities along roll, pitch and yaw directions. Velocity contours and streamline plots for CFD simulations are shown in Figure 3. Values of all six forces and moments against every translational and rotational velocities were tabulated and used for estimation of damping coefficients.

Quadratic fit between damping forces during translations is shown in Figure 4. For instance, the coefficients along heave direction can be estimated using the fit as $Z_w w + Z_{w|w|} w|w|$, where Z_w and $Z_{w|w|}$ are linear and quadratic damping coefficients respectively. A similar approach was adopted to estimate other direct and cross coupled coefficients with approximations. Due to asymmetric outer profile of *Acutus*, forces are not same for equal positive and negative velocities, which is evident from Figure 4.

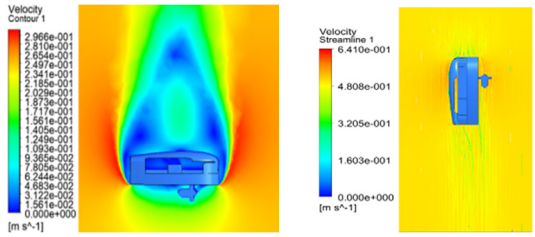

(a) (b)

Figure 3: (a) Velocity contours for 0.5m/s flow velocity along negative Z_B and (b) Streamlines for 0.5m/s flow velocity along negative X_B.

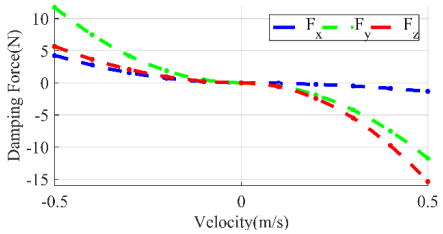

Figure 4: Variation of damping forces along X_B, Y_B, Z_B.

3.2 Parameter Estimation for Control Plane and Thruster Dynamics

Dynamics of control planes and water thruster are modelled as the external forces and moments to the fuselage system. External force and moment vector $\boldsymbol{\tau}$ in (1) are sum of forces and moments from two flaps, rudder and thruster. Thruster produces a force along surge direction and a reaction torque along the roll axis. Thrust and torque versus input voltage data is used to model the thruster.

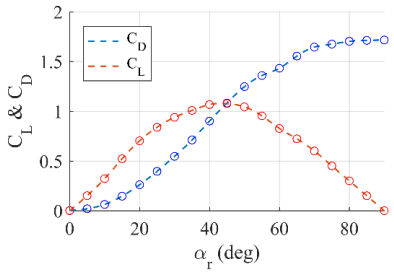

Figure 5: Variation of C_L and C_D against α for rudder.

CFD simulations of rudder and flaps against various flow angles are conducted to record the drag force (F_d) and lift force (F_l) versus angle of attack (α). Using equations as shown in (2), coefficients of drag (C_D) and coefficient of lift (C_L) are estimated against α ranging from 0° to 90° for flow velocity of up to 0.5m/s and gauge pressure of 1 bar. ρ is density of water and A is area of the rudder plate. V is the relative velocity w.r.to the flow.

$$F_d = \frac{1}{2}\rho C_D A V|V| \text{ and } F_l = \frac{1}{2}\rho C_L A V|V| \quad (2)$$

Surge velocity (u) and sway velocity (v) are resolved into u_0 and v_0 along rudder and its perpendicular direction respectively as described in the (3) and (4).

$$u_0 = u\cos\theta_r - v\sin\theta_r \quad (3)$$

$$v_0 = u\sin\theta_r + v\cos\theta_r \quad (4)$$

Rudder angle of attack (α_r) and relative velocity (V) can be calculated as shown in (5) and (6) respectively. C_D and C_L for a rudder angle is estimated from look up table modelled from data as shown in Figure 5. Fuselage angle of attack (β_r) is given by the expression as shown in (7).

$$\alpha_r = tan^{-1}\left(\frac{u_0}{v_0}\right) \quad (5)$$

$$V = u_0\cos\alpha_r + v_0\sin\alpha_r \quad (6)$$

$$\beta_r = tan^{-1}\left(\frac{u}{v}\right) \quad (7)$$

Forces generated by rudder can be calculated by resolving the components of F_d and F_l along X_B and Y_B. Drag (F_d) is always anti-parallel to relative flow velocity V and the lift (F_l) can change directions for different cases of sign of u_0 and v_0. For the case with positive u_0 and v_0, the relationship between the above said forces can be represented in matrix form as,

$$\begin{bmatrix}F_x\\F_y\end{bmatrix} = \begin{bmatrix}-cos\,\beta_r & sin\,\beta_r\\ -sin\,\beta_r & -cos\,\beta_r\end{bmatrix}\begin{bmatrix}F_d\\F_l\end{bmatrix} \quad (8)$$

Rudder produces roll, pitch and yaw moments about the COG due to the offset of point of application of forces along all three axes. Centre of gravity on the trapezium shaped flat surface can be assumed as centre of pressure (CP) for rudder. F_x and F_y act at CP which is at a distance r_z along Z_B from COG. The distance between COG and axis of rotation of rudder along X_B is r_x, and perpendicular distance between CP and axis of rotation is a. Yaw moment produced by rudder has a significant effect on rotation of the fuselage in the yaw direction and coupled sway motion. Moments about X_B, Y_B, Z_B are calculated as shown in (9).

$$\begin{bmatrix}M_{roll}\\M_{pitch}\\M_{yaw}\end{bmatrix} = \begin{bmatrix}-F_y\,r_z\\F_x\,r_z\\F_x\,a\,sin(\beta_r) + F_y\,(a\,cos(\beta_r)r_x)\end{bmatrix} \quad (9)$$

$$\boldsymbol{\tau} = \boldsymbol{\tau_{rudder}} + \boldsymbol{\tau_{rightflap}} + \boldsymbol{\tau_{leftflap}} + \boldsymbol{\tau_{thruster}} \quad (10)$$

Vector of forces and moments due to rudder is represented as $\boldsymbol{\tau_{rudder}} = [F_x\,F_y\,F_z\,M_{roll}\,M_{pitch}\,M_{yaw}]^T$. A similar method can be adopted to calculate forces and moments vector for thruster, right and left flaps

represented by $\boldsymbol{\tau_{thruster}}$, $\boldsymbol{\tau_{rightflap}}$ and $\boldsymbol{\tau_{leftflap}}$ respectively. Net forces and moments vector can be expressed as a sum of these vectors by neglecting external disturbances in water as shown in (10).

3.3 Aerial Dynamics and Controller

As discussed earlier, *Acutus* reconfigures itself to a quadrotor during its navigation in air. A mathematical model has been developed for aerial operation of *Acutus* based on dynamics of quadrotor derived in (Bouabdallah et al, 2004). The convention for body and global frame coordinate axes is the same as discussed in section 3.1. Modelling of quadrotor dynamics and controller design for multirotor systems has been a topic of wide and active research. The aerial dynamics of the robot can be expressed using Newton-Euler formalism similar to (1) by simply eliminating the added mass and hydrodynamic drag terms for aerial dynamics. Buoyancy terms in restoring forces and moments vector $\boldsymbol{g}$ are set to zero for aerial model. The overall dynamics of aerial system can be represented as shown in (11a).

$$\mathbf{F}_a(\mathbf{M_{rb}}, \mathbf{C_{rb}}, \boldsymbol{g}, \boldsymbol{\eta}, \dot{\boldsymbol{\eta}}, \ddot{\boldsymbol{\eta}}, \Omega) = \boldsymbol{\tau_a}(\boldsymbol{U_{1-4}}, \boldsymbol{\Omega_{1-4}}) \quad (11a)$$

$$\Omega = \Omega_2 + \Omega_4 - \Omega_1 - \Omega_3 \quad (11b)$$

The system inputs U_1, U_2, U_3, U_4 are functions of rotor speeds Ω_1, Ω_2, Ω_3, Ω_4. Disturbance Ω is function of these speeds as defined in (11b). Torque applied on the body of vehicle along an axis is difference between the torque generated by each propeller on other axis and can be expressed as functions of rotor speeds (Bouabdallah et al, 2004).

A cascaded PI-PID controller as available on commercial autopilots was implemented for stabilization of the experimental quadrotor system in aerial traversal as proposed in (Nandakumar et al, 2017).

The models of aerial and underwater systems can be combined as shown in (12a). Here, ζ is the switching variable using which these dynamics are switched based on the rule shown in (12b).

$$\begin{aligned}&\zeta\mathbf{F}_a(\mathbf{M_{rb}}, \mathbf{C_{rb}}, \boldsymbol{g}, \boldsymbol{\eta}, \dot{\boldsymbol{\eta}}, \ddot{\boldsymbol{\eta}}, \Omega) + (1\\ &-\zeta)\ \mathbf{F}_u(\mathbf{M}, \mathbf{C}, \mathbf{D}, \boldsymbol{g}, \dot{\boldsymbol{\nu}}, \boldsymbol{\nu}, \boldsymbol{\eta})\\ &= \zeta\boldsymbol{\tau_a}(\boldsymbol{U_{1-4}}, \boldsymbol{\Omega_{1-4}}) + (1\text{-}\zeta)\boldsymbol{\tau_u}\end{aligned} \quad (12a)$$

$$\zeta = \begin{cases} 1; \text{ if } z < 0 \\ 0; \text{ otherwise} \end{cases} \quad (12b)$$

4 SIMULATIONS AND RESULTS

Numerical simulations have been carried out for various input conditions in *MATLAB* Simulink for aerial, underwater navigation and transition. Simulation results are used to validate the design and developed mathematical model, analyse the performance of the system in different modes of operation.

Zig-Zag manoeuvre is a standard test performed to evaluate the zig-zag manoeuvrability, course-keeping ability and underwater vehicle's response to rudder (Issac et al., 2008), (Yu et al, 2014). The zigzag manoeuvre for robot is obtained by varying rudder angle (θ_r) between -θ_{max} and θ_{max}. Simulation results for a zigzag manoeuvre of *Acutus* at 75% of maximum thrust (~38*N*) are shown in Figure 6. Due to offset between COG and COB along X_B, a pitch of -9° is observed in the robot.

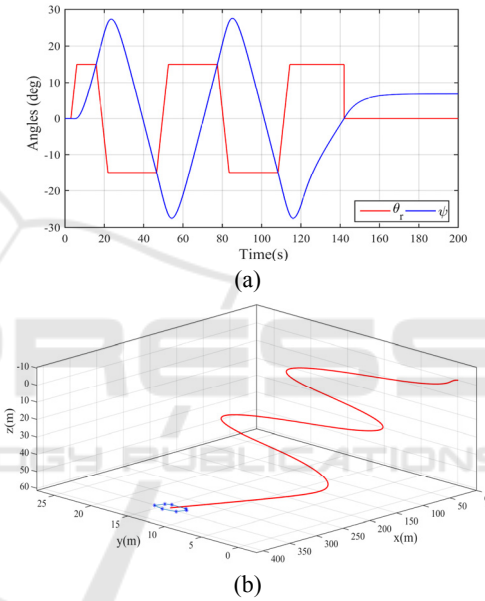

Figure 6: Simulation results for 15° / 15° zigzag manoeuvre (a) Rudder input (θ_r) and yaw (ψ) (b) 3D trajectory of the zigzag manoeuvre.

Pitch manoeuvrability of the robot can be understood from simulation results for varying pitch input under constant thrust as shown in Figure 7. The robot was found to achieve high surge velocities up to 2*m/s* at 75% of maximum thrust owing to the streamlined profile.

Another test to evaluate the turning and course changing ability of marine vehicles is turning circle test and steady turning diameter acts as a quantitative measure for steering manoeuvrability. Variation of steady turning diameter against different rudder angles under 75% maximum thrust is shown in Figure 8. Inherent pitch in the underwater system induces a coupled heave motion despite zero flap angle. Therefore, the system is observed to descend with a

constant heave velocity tracing a helix with steady turning diameter of ~87.3m for 35° rudder angle as shown in Figure 8(c).

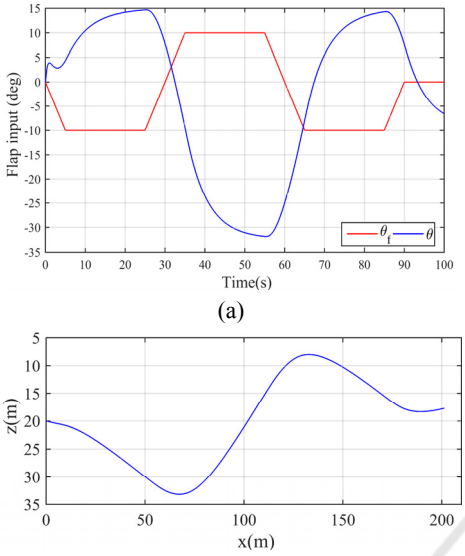

Figure 7: (a) Flap input (θ_f) and pitch (θ) (b) Path traced by robot over time.

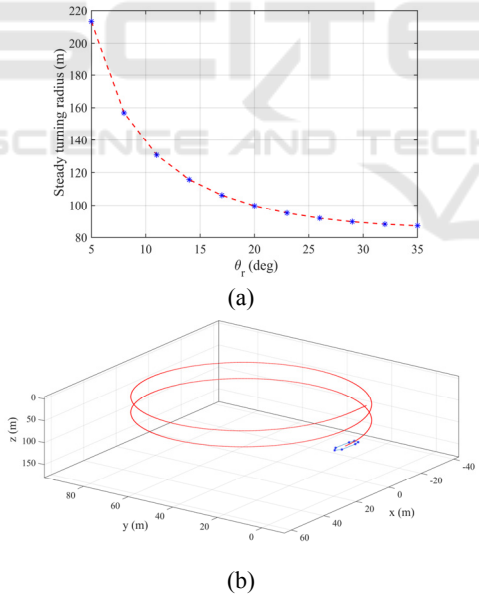

Figure 8: (a) Steady turning diameter versus rudder input (θ_r) (b) Helical path traced by robot at constant thrust and 35° rudder angle.

Numerical simulations for complete sequence of water to air and air to water traversal have been conducted to understand the operation at transition phase. Simulation results for water to air traversal are shown in Figure 9. Underwater traversal is executed for a duration of 32.5s. Transition is the intermediate state occurring at z = 0m, where the mathematical model switches from underwater dynamics to aerial dynamics. Aerial traversal commences system after a delay of 2.5s for retraction of the arms. Performance of the tuned aerial controller was observed to be satisfactory as demonstrated in Figure 9(b). Path traced by robot in $X_G Z_G$ plane starting from (0, 0, 5m) is shown in Figure 9(c).

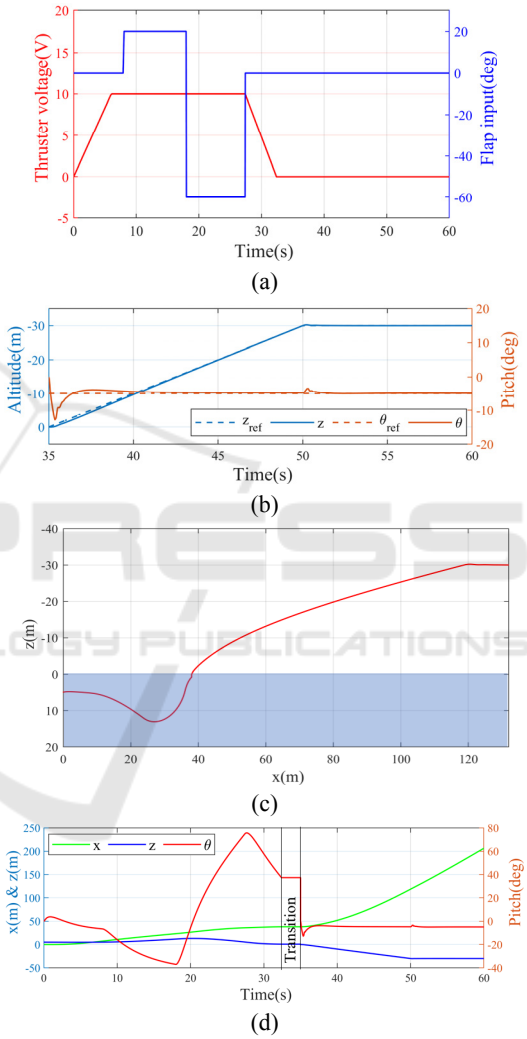

Figure 9: (a) Thruster voltage input and flap angle input for underwater traversal (b) Desired and actual altitude for aerial traversal starting at t = 35s (c) Trajectory of water to air traversal for above inputs (d) Variation of position along X_G & Z_G axis, and pitch (θ).

Simulation results for air to water traversal are shown in Figure 10. Aerial traversal is executed for a duration of 8s with a constant pitch reference of -1°. Delay of 2s has been introduced at transition phase for retraction of arms. Underwater traversal

commences after the delay with varying thruster voltage and flap angle inputs as shown in Figure 10(a). Path traced by robot in $X_G Z_G$ plane starting from $4m$ above water is shown in Figure 10(c).

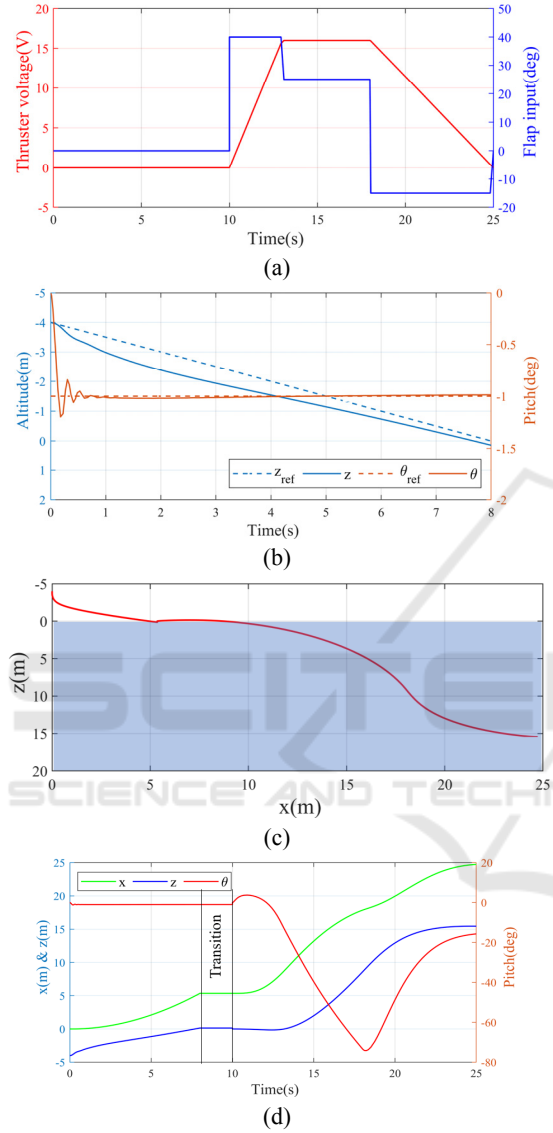

Figure 10: (a) Thruster voltage input and flap angle input starting at t = 10s (b) Desired and actual altitude for aerial traversal (c) Trajectory of air to water traversal for above inputs (d) Variation of position along X_G & Z_G axis, and pitch (θ).

5 EXPERIMENTAL SETUP

An experimental setup of the vehicle has been developed after multiple design iterations and simulation studies. The weight of the designed prototype is 77N and the buoyancy is 78N. Hence, the residual buoyancy is 1N underwater. For internal stability of the quadrotor, COG of the system has been adjusted to be below the centre of rectangle formed by aerial rotors in their extended position. Metallic body (capsule) is made of stainless steel and houses electronics while providing a strong skeleton to support all the on-board components. The capsule is 0.62m long, 0.2m wide and can withstand a pressure up to 10m underwater. A 3D printed shroud has been used for streamlining the flow. Shroud is fixed on top of the capsule and contains slots for passage of aerial rotors and propellers during retraction. Aluminium channels of suitable dimension were chosen as structural members for retracting arms based on FEA studies and cantilever bending load calculations.

Three high torque metal gear servo motors are used to drive the shafts of rudder and two flaps. Two micro speed reduction metal gear box DC motors drive the worm gear for retraction of the quadrotor arms. A combination of 4 BLDC motors with a maximum thrust of 45N each, 16x5.4-inch carbon fibre propellers and 60A electronic speed controllers (ESCs) have been chosen for aerial propulsion. The water thruster can provide a maximum thrust of up to 50N. Underwater system is equipped with a pressure sensor and a 9 DOF Inertial Measurement Unit (IMU). Communications with the user console happens over a neutrally buoyant long tether. Aerial electronic architecture consists of a standard flight controller and radio system embedded with accelerometer and gyroscope. PI-PID controller is being used for aerial operation. The prototype is being tested for underwater traversal and aerial-aquatic transition.

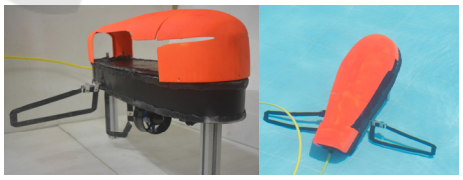

Figure 11: Experimental prototype (work in progress).

6 CONCLUSION

A hybrid aerial-underwater robot has been conceptually designed and the same has been mathematically modelled to analyse the behaviour. Simulations were carried out to demonstrate the capabilities. The results prove the concept and shows that such robots can be used for multiple applications.

A prototype has been developed after iterative improvisations based on the simulation results and the same is being tested. The work presented in this paper is an analysis of design, parameter estimation and dynamic model of the system. Further study on the coupled underwater dynamics and closed loop analysis of the coupled system are ongoing.

REFERENCES

Ai, X., Kang, S. and Chou, W. (2018) 'System Design and Experiment of the Hybrid Underwater Vehicle', in *2018 International Conference on Control and Robots (ICCR)*. Hong Kong, China: IEEE, pp. 68–72.

Alzu'bi, H., Mansour, I. and Rawashdeh, O. (2018) 'Loon Copter: Implementation of a hybrid unmanned aquatic–aerial quadcopter with active buoyancy control', *Journal of Field Robotics*, 35(5), pp. 764–778. doi: 10.1002/rob.21777.

Bouabdallah, S., Murrieri, P. and Siegwart, R. (2004) 'Design and control of an indoor micro quadrotor', in *IEEE International Conference on Robotics and Automation, 2004. Proceedings. ICRA '04. 2004*. Los Angels, USA, p. 4393–4398 Vol.5. doi: 10.1109/ROBOT.2004.1302409.

Bouabdallah, S. and Siegwart, R. (2006) *Dynamic Modeling of Fixed-Wing UAVs*, *Swiss Federal institute of technology,version 2*.

Caccia, M., Indiveri, G. and Veruggio, G. (2000) 'Modeling and identification of open-frame variable configuration unmanned underwater vehicles', *IEEE Journal of Oceanic Engineering*, 25(2), pp. 227–240.

Crespi, A. and Ijspeert, A. J. (2005) 'Swimming and Crawling with an Amphibious Snake Robot', in *Proceedings of the 2005 IEEE International Conference on Robotics and Automation*. Barcelona, Spain, pp. 24–28.

Crespi, A., Karakasiliotis, K. and Ijspeert, A. J. (2013) 'Salamandra Robotica II : An Amphibious Walking Gaits', *IEEE Transactions on Robotics*, 29(2), pp. 308–320.

Fernando, H. C. T. E., Silva, D. and Munasinghe, S. R. (2013) 'Modelling , Simulation and Implementation of a Quadrotor UAV', in *IEEE International Conference on Industrial and Information Systems*. Peradeniya, Sri Lanka. doi: 10.1109/ICIInfS.2013.6731982.

Fossen, T. I. (2011) *Handbook of Marine Craft Hydrodynamics and Motion Control*. 1st edn, *Handbook of Marine Craft Hydrodynamics and Motion Control*. 1st edn. doi: 10.1002/9781119994138.

Iisu, P. et al. (1987) 'Adaptive Identification and Control', in *IEEE International Conference on Robotics and Automation*. Raleigh, USA, pp. 1210–1215.

Issac, M. T. et al. (2008) 'Analysis of Horizontal Zigzag Manoeuvring Trials from the MUN Explorer AUV', in *Oceans 2008*. Kobe, Japan.

Khan, W. and Nahon, M. (2016) 'Modelling Dynamics of Agile Fixed-Wing UAVs for Real-Time Applications', in *International Conference on Unmanned Aircraft Systems*. Arlington, USA, pp. 1303–1312. doi: 10.1109/ICUAS.2016.7502599.

Kurak, S. and Hodzic, M. (2018) 'Control and Estimation of a Quadcopter Dynamical Model', *Periodicals of Engineering and Natural Sciences*, 6(1), pp. 63–75. doi: 10.21533/pen.v6i1.164.

Michael, N. et al. (2014) 'Collaborative Mapping of an Earthquake Damaged Building via Ground and Aerial Robots', *Journal of Field Robotics*, pp. 33–47. doi: 10.1007/978-3-642-40686-7.

Nandakumar, G., Srinivasan, A. and Thondiyath, A. (2017) 'Theoretical and Experimental Investigations on the Effect of Overlap and Offset on the Design of a Novel Quadrotor Configuration , VOOPS', *Journal of Intelligent Robotic Systems*. Journal of Intelligent & Robotic Systems.

Ranganathan, T. et al. (2018) 'Design and Analysis of a Novel Underwater Glider – RoBuoy', in *International Conference on Robotics and Automation (ICRA)*. Brisbane, Australia.

Slotine, J.-J. E. and Li, W. (1989) 'Composite adaptive control of robot manipulators', *Automatica*, 25(4), pp. 509–519. doi: 10.1016/0005-1098(89)90094-0.

Smallwood, D. A. and Whitcomb, L. L. (2003) 'Adaptive identification of dynamically positioned underwater robotic vehicles', *IEEE Transactions on Control Systems Technology*, 11(4), pp. 505–515.

Stewart, W. et al. (2018) 'Design and demonstration of a seabird-inspired fixed-wing hybrid UAV-UUV system Design and demonstration of a seabird-inspired fixed-wing hybrid UAV-UUV system', *Bioinspiration & Biomimetics*. IOP Publishing.

Szymak, P. (2016) 'Mathematical model of underwater vehicle with undulating propulsion', in *2016 Third International Conference on Mathematics and Computers in Sciences and in Industry (MCSI)*. *IEEE*, pp. 269–274. doi: 10.1109/MCSI.2016.057.

Wales, N. S. (1986) 'Adaptive computed torque control for rigid link manipulators', in *Conference on Decision and Control*. Athens, Greece, pp. 68–73.

Wang, B. et al. (2009) 'Modeling and motion control system research of a mini underwater vehicle', in *2009 International Conference on Mechatronics and Automation*. Changchun, China: *IEEE*, pp. 4463–4467. doi: 10.1109/ICMA.2009.5244851.

Yu, C., Xiang, X. and Zhao, R. (2014) 'Horizontal Zigzag Maneuverability of UUV in Limited Space', in *Chinese Control and Decision Conference*. Changsha, China, pp. 3306–3310.

Zhang, X. et al. (2014) 'A Survey of Modelling and Identification of Quadrotor Robot', *Abstract and Applied Analysis*, 2014.